AAPS PharmSciTech, Vol. 14, No. 2, June 2013 (© 2013)
DOI: 10.1208/s12249-013-9965-x

Research Article

Electrospun Chitosan Microspheres for Complete Encapsulation of Anionic Proteins: Controlling Particle Size and Encapsulation Efficiency

Ji Suk Choi,[1,2] Younghee Kim,[1] Jihyun Kang,[1] Seo Young Jeong,[3,4] and Hyuk Sang Yoo[1,2,4]

Received 4 December 2012; accepted 30 March 2013; published online 30 April 2013

Abstract. Electrospinning was employed to fabricate chitosan microspheres by a single-step encapsulation of proteins without organic solvents. Chitosan in acetic acid was electrospun toward a grounded sodium carbonate solution at various electric potential and feeding rates. Electrospun microspheres became insoluble and solidified in the sodium carbonate solution by neutralization of chitosan acetate. When the freeze-dried microspheres were examined by scanning electron microscopy, the small particle size was obtained at higher voltages. This is explained by the chitosan droplet size at the electrospinning needle was clearly controllable by the electric potential. The recovery yield of chitosan microspheres was dependent on the concentration of chitosan solution due to the viscosity is the major factor affecting formation of chitosan droplet during curling of the electrospinning jets. For protein encapsulation, fluorescently labeled bovine serum albumin (BSA) was codissolved with chitosan in the solution and electrospun. At higher concentration of sodium carbonate solution and longer solidification time in the solution, the encapsulation efficiency of the protein was confirmed to be significantly high. The high encapsulation efficiency was achievable by instant solidification of microspheres and electrostatic interactions between chitosan and BSA. Release profiles of BSA from the microspheres showed that the protein release was faster in acidic solution due to dissolution of chitosan. Reversed-phase chromatography of the released fractions confirmed that exposure of BSA to acidic solution during the electrospinning did not result in structural changes of the encapsulated protein.

KEY WORDS: chitosan; electrospinning; encapsulation; microspheres; protein.

INTRODUCTION

Polymeric microspheres have been conventionally employed as drug delivery reservoirs for peptides and proteins because sustained release of the encapsulated drugs can be obtained with the injectable matrix (1–3). For fabrication of protein-encapsulated microspheres, emulsification of immiscible solvents were widely employed to incorporate amphiphilic proteins within hydrophobic matrix of the polymeric carriers. Proteins solutions emulsified in organic phase were double-emulsified in aqueous phase to form a water-in-oil-in-water (W/O/W) emulsion or protein dispersed in organic solvents were emulsified in aqueous phase to form an oil-in-water emulsion (O/W) (4,5). Thus, various emulsifiers have been employed to stabilize the multiple interfaces between two immiscible solvents, such as PVA and Tween® (nonionic polyoxyethylene surfactants), whose biocompatibility was not yet elucidated for *in vivo* applications (6,7). Therefore, several studies have been employing alternative strategies such as a melt dispersion method and an emulsifier-free emulsion method to eliminate or avoid the use of those surfactants for fabrication of microspheres (8,9). Electrospray techniques eject polymer solutions through an atomizer under high pressures and the sprayed polymeric solutions dries under a cyclone of hot gas (10,11). This has been a useful technique to prepare microparticles encapsulating bioactive proteins, however, the loading efficiency were considerably low because the protein should be codispersed with the matrix polymer in organic solvents.

Chitosan, a cationic polysaccharide composed of β-(1-4)-linked D-glucosamine and *N*-acetyl-D-glucosamine, has been extensively studied for biomedical applications because of superior biocompatibility and inexpensiveness compared to synthetic polymers. Although chitosan and chitosan derivatives have been widely formulated into nanoparticles for drug delivery (12–15), fabrication of chitosan microspheres (CMs) was not actively studied because deprotonated amine groups of chitosan decrease water solubility in neutral environment (16). Most CMs have been prepared by emulsification and spray drying techniques. Chitosan dissolved in acidic solution was directly dropped into organic phase for water-in-oil (W/O) emulsifications, which was followed by chemical cross-linking of chitosan for solidification (17,18). However, chemically cross-linked chitosan is rarely solubilized in

[1] Department of Biomaterials Engineering, Kangwon National University, Chuncheon, Republic of Korea 200-701.
[2] Institute of Bioscience and Bioengineering, Kangwon National University, Chuncheon, Republic of Korea.
[3] College of Pharmacy, Kyung Hee University, Seoul, Republic of Korea.
[4] To whom correspondence should be addressed. (e-mail: hsyoo@kangwon.ac.kr; e-mail: syjeong@khu.ac.kr)

aqueous phase and degradation of CMs is significantly restricted. In order to avoid the chemical medication of chitosan, noncross-linked CMs were widely fabricated by spray-drying techniques. While monodispersed particle size distribution of CMs was obtained by spray-drying techniques, expensive equipment, and low encapsulation efficiency of protein have been bottlenecks for further commercialization (19–21).

As an alternative strategy, electrospinning, the curling of electrically charged jets, has been widely employed as a valuable tool of fabricating nonwoven fibrous meshes with micro- or nanoscales. Because of the simplicity of the fiber drawing process, various polymeric solutions were electrospun to prepare micro- and nano-porous polymeric fibrous sheets for textile industry, tissue engineering, and drug delivery (22–25). Previously, we electrospun biocompatible polymers to encapsulate and immobilize bioactive proteins in the fibrous meshes for controlled release of the incorporated proteins (26–28). Protein in aqueous phase was co-electrospun with the organic phase containing polymers through a dual nozzle to encapsulate the protein within the core of the nanofiber. The core-encapsulated proteins were rapidly released out from the fibrous matrix and the surface-immobilized proteins were rarely released out from the single meshes; however, the immobilized protein continuously stimulated cellular signals from an extend periods. We speculated that the encapsulated protein at the core was released out through the very thin shells of the nanofiber by diffusion. More commonly, many researchers are frequently dispersing proteins in organic phase containing polymers mixtures to obtain electrospun nanofibers (29). However, the protein was not homogeneously encapsulated within the fibers due to phase separation between the polymeric phase and proteins during the electrospinning process; this subsequently caused undesirable release profiles of the protein such as nonrelease or initial burst release behaviors.

In the current study, we fabricated protein-encapsulating CMs by electrospinning and subsequent solidification in sodium carbonate solutions. Chitosan solution was electrospun at various conditions such as various electric potentials, viscosities, ejecting speeds, and solidification rates. We also investigated protein encapsulation behaviors of the CMs with fluorescently labeled proteins and tracked down the release profiles of the encapsulated protein according to pH changes.

MATERIALS AND METHODS

Materials

Chitosan (Mw 50 kDa) was purchased from Wako Chemical Co. (Japan). Bovine serum albumin (BSA) and fluorescein isothiocyanate isomer (FITC) were obtained from Bio Basic, Inc. (Canada) and Sigma (Saint Louis, MO, USA), respectively. Glacial acetic acid and trifluoroacid (TFA) were purchased from Daejung Chemical (Korea). Sodium carbonate (Na_2CO_3) and hydrochloric acid (HCl) were obtained from Junsei (Japan). Acetonitrile were purchased from and JT Baker Inc. (Phillipsburg, NJ, USA). All chemicals were used of analytical grades.

Preparation of CMs by Electrospinning

CMs were prepared by electrospinning with a minor modification. Chitosan was completely dissolved in 0.2 M acetic acid with various concentrations (1.0, 2.0, and 3.0% (*w*/*v*)), then, chitosan solution was injected through 25G needles at various flow rates (0.5, 1.0, and 2.0 ml/h). The voltage differences and the distance between a ground and a needle were 2.5–10.0 kV and 5.5 cm, respectively. Chitosan droplets at the tip of the needle were electrospun into Na_2CO_3 (0.5 M–4.0 M) with gentle stirring at 60 rpm for immediate solidification. The solidified CMs were filtered through a nylon mesh, washed five times with distilled water, and lyophilized. In order to estimate a recovery yield of CMs, CMs in Na_2CO_3 were collected after electrospinning for 2 h, and then the CMs were transferred into 50-mL conical tube after neutralization and washing. After lyophilization, the 50-mL conical tube containing CMs was weighted. For confirmation morphology of CMs, the lyophilized microspheres on a specimen mount were sputter-coated with a gold palladium and examined by a field emission-scanning electron microscopy at the central lab of the Kangwon National University (FE-SEM, S-4300, Hitachi, Japan). The average diameters of the CMs were measured with the SEM images by an image-analyzing software (DIXI Images Solution, Korea; n=10).

Preparation of FITC–BSA-Loaded CMs

In order to visualize the encapsulated BSA within CMs, BSA labeled with FITC was encapsulated in CMs. Briefly, 0.5 mL of FITC in acetone (1.0 mg/ml) was slowly added into 10.0 mL of BSA in 0.1 M Na_2CO_3 (1 mg/ml) and reacted at 4°C in the dark for 8 h. Unreacted FITC was completely removed by dialysis (SpectroPor, MW cutoff=50,000) and FITC–BSA was lyophilized. For preparing FITC–BSA-loaded CMs, FITC–BSA added into chitosan solution in 0.2 M acetic acid. Then weight ratio of FITC–BSA to chitosan was 1 to 100. After completely dissolving FITC–BSA in chitosan solution, the FITC–BSA/chitosan solution was electrospun at various flow rates (0.5, 1.0, and 2.0 ml/h). The voltage differences and the distance between a ground and a needle were 2.5–10.0 kV and 5.5 cm, respectively. Chitosan droplets at the tip of the needle were electrospun into Na_2CO_3 (0.5–4.0 M) with gentle stirring at 60 rpm for immediate solidification. The solidified CMs were filtered through a nylon mesh, washed five times with distilled water to remove FITC–BSA on surface of CMs. FITC–BSA within CMs was visualized by confocal laser scanning microscopy (FV300, Olympus, Japan). FITC–BSA-encapsulating CMs were placed on a glass slide and a mounting medium was added to fix a cover slip. FITC–BSA in the CM was excited at 488 nm and the emission filters were set for FITC detection (bp. 505–525 nm).

Encapsulation Efficiencies of FITC–BSA in CMs

In order to determine an actual amount of the encapsulated FITC–BSA in the CMs, a fluorescence intensity of FITC–BSA was measured to quantification of the FITC–BSA in CMs after solvent extraction. Briefly, after washing FITC–BSA-encapsulating CMs, the FITC–BSA-encapsulating CMs (5.0 mg) were completely dissolved in 1.0 M HCl with vigorous vortexing at room temperature for 24 h

and centrifuged at 10,000 rpm for 15 min. A fluorescence intensity of the supernatant was measured by spectrofluorometry (λ_{ex}=490 nm, λ_{em}=520 nm; F-2500, Hitachi, Japan). FITC–BSA was used as a standard for a calibration curve (0–200 μg/ml). The encapsulation efficiency was calculated as follows:

$$\textit{Encapsulation efficiency}(\%, w/w) = ((\textit{the actual amount of encapsulated FITC}-\textit{BSA in the CMs})/(\textit{the theoretical amount of FITC}-\textit{BSA in the CMs})) \times 100$$

In Vitro Release Profiles of FITC–BSA from the CMs

Release behaviors of FITC–BSA from the CMs were monitored at various pHs (pH 3.0–8.4). The CMs (5.0 mg) were dispersed in 5 mL of 10 mM citric buffers (pH 3.0 and 5.5) and phosphate buffered saline (PBS, pH 7.0 and 8.4). Then, the CMs in each buffer were incubated with vigorous shaking at 250 rpm with 37°C for 24 h. At predetermined time, the CMs were centrifuged at 10,000 *g* for 15 min. The supernatants were measured to quantify the amount of released FITC–BSA by spectrofluoremetry. The amount of the released FITC–BSA in the CMs was calculated using the following equation:

$$\textit{Cumulative release}(\%, w/w) = (\textit{the amount of released FITC}-\textit{BSA from the CMs})/(\textit{the actual amount of encapsulated FITC}-\textit{BSA in the CMs})) \times 100$$

Stability of the Released FITC–BSA

The fractions of released FITC–BSA from the CMs were analyzed by reversed phase high pressure liquid chromatography (RP-HPLC) system equipped with a Jupiter C18 column (250×4.6 mm, 5 μ, 300 Å). The mobile phase, a mixture of water and acetonitrile (90:10) with 0.01% TFA, was flowed at flow rate of 1.0 ml/min at ambient temperature. Twenty microliters of the fractions of released FITC–BSA were injected to the RP-HPLC system and the signals were gained by a UV detector at 280 nm. FITC–BSA in PBS (1 mg/ml, pH 6.9) was used as a control.

Statistical Analysis

All the results are expressed in mean values±standard deviation. The statistical significance between a pair of groups was determined by conducting a one-way ANOVA with Sigma plot 12.0 software (SPSS); a value of $p<0.05$ was considered statistically significant.

RESULTS AND DISCUSSION

Figure 1 shows a schematic presentation of preparing CMs by an electrospinning process. Chitosan dissolved in acetic acid was ejected and electrospun to the grounded Na_2CO_3solution for neutralization of chitosan. Chitosan, a positively-charged natural polymer, was solubilized in acetic acid and the acetate ion was bound to the protonated amine groups by electrostatic interactions (30,31). For solidification of CMs, the acetate groups need to be scavenged at high pH, where the primary amine groups of the chitosan are deprotonated. After electrospinning of the chitosan solution into the grounded Na_2CO_3 solution, the semi-solidified chitosan solution was neutralized in Na_2CO_3solution at pH; this gradually solidifies the droplet of the chitosan solution because the deprotonation of chitosan (pKa=~6.5) occurs at the higher pHs. Previously, electrospun chitosan nanofibrous meshes were prepared with neutralization of chitosan nanofibers in the saturated Na_2CO_3 solution to prevent dissolution of chitosan nanofibers (32). The neutralized nanofibrous meshes became insoluble in an aqueous phase and the fibrous structures were maintained due to the neutralization process. Thus, in the current study, we further speculate that the solidification process can be controlled both by a concentration of Na_2CO_3 and the incubation period for the hardening process.

Figure 2 shows the formation of CMs in various chitosan concentrations and electrospinning voltages. As shown in Fig. 2a, the electrospinning voltages significantly affected morphology of the CMs; at 10 kV, the microspheres were not fabricated while micron-sized spheres were obtained for 2.5 and 5.0 kV. Several studies previously indicated that fiber diameters could be controlled by changing electrospinning voltages (33–35). Electrospinning is sputtering and curling of charged jets upon voltage differences. Thus, the rupture of the polymeric cone at the tip of the electrospinning needle is controlled by a delicate balance between the surface tension of polymeric solutions and the electrospinning voltages; the higher voltages result in faster ruptures of the polymeric cone.

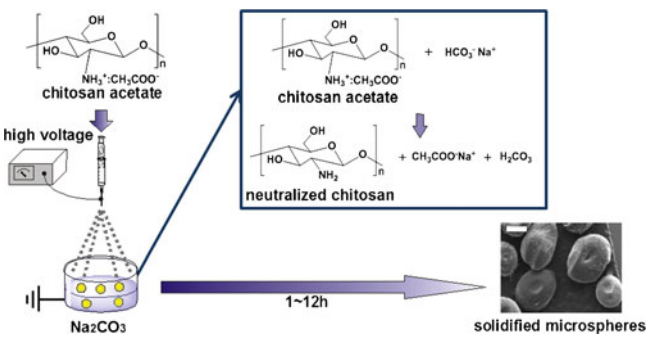

Fig. 1. Schematic presentation of preparing chitosan microspheres (CMs) by electrospinning. The charged polymer jets were electrospun to the grounded Na_2CO_3 and further solidified by neutralization of chitosan acetate with Na_2CO_3. The *scale bar* in the image is 500 μm

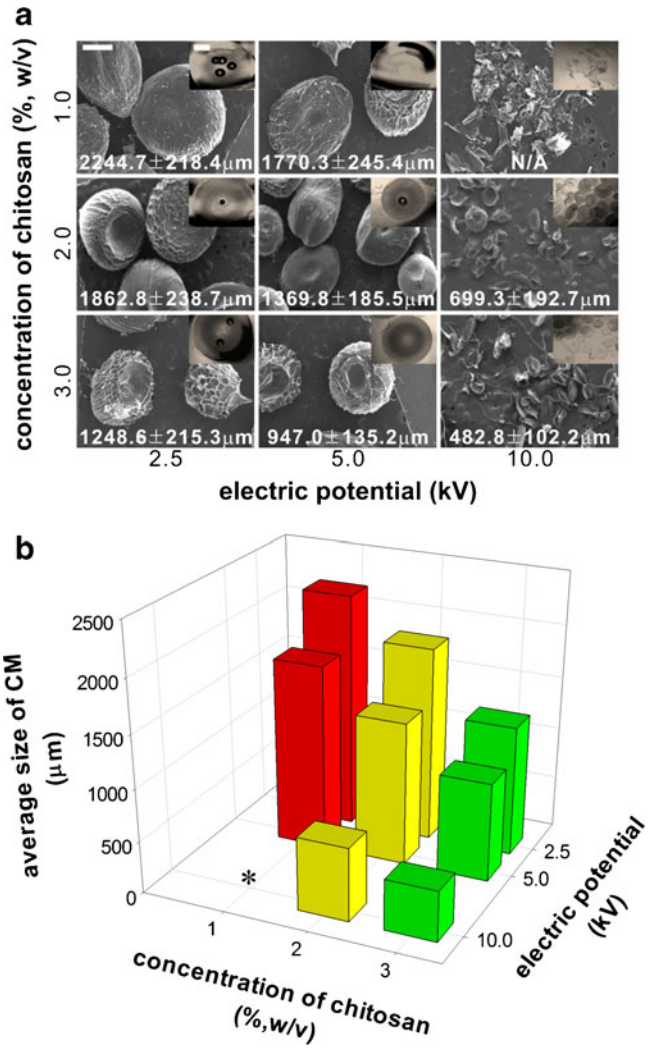

Fig. 2. Fabrication of CMs with various concentrations of chitosan solutions and electric potential for electrospinning at 2.0 ml/h of a constant feeding rate. **a** SEM of the CMs after solidification and the insets in the SEM image are the optical microscopic images of CMs before lyophilization. **b** Average diameters of CMs based on an image analysis of the SEM images. The average sizes were plotted against the concentrations of chitosan and the electric potentials (n=10). All *scale bars* in the images are 500 μm. *Asterisks* average size of CMs was not measured due to irregular shapes of the CMs

The mass of the curling jets subsequently reduces compared to those with slower ruptures of the polymeric jets. Thus, many researchers observed that the decrease of fiber diameters when electrospinning voltages increased (36,37). Similarly, we observed that attenuated ruptures of the charged jet at lower voltages were advantageous for fabricating micron-size microspheres. At the lower electric potentials, the mass of the charged polymer jets are clearly increased compared to those with higher potentials, suggesting the size of electrospun particles can be significantly increased accordingly. Also, a high surface tension of polymeric solution could support faster ruptures of the polymeric jets. Thus, when a concentration of chitosan was 3.0%, the size of CMs was smaller than those of 1.0 and 2.0% chitosan because the surface tension was increased as increasing the concentration of polymeric solution. Moreover, acetic acid that was used to dissolve the chitosan supported the increase of the conductivity of the chitosan solution because the acetic acid is a strong acid (38). Additionally, the CMs are "donut-like" shaped, the concave surface at the core of CMs. Because the charged jets of chitosan solutions were withdrawn by the ground, the shape tends to be ellipsoidal shapes rather than perfect round shapes (Fig. 2a). Thus, un-neutralized chitosan at the core of the microspheres is easily dissolved by the surround water phase compared to the round shaped microspheres. We believe that this effect resulted in the interesting shape of the CMs.

Figure 3 showed the captured images of the droplet at the tip of the needle at the moment that the droplets were ejected to the ground. According to the applied electric potential for electrospinning, various morphologies of chitosan droplets were observed at the tip of the needle. When the electric potential increased from 0 to 10 kV, the size and the shape of the droplet become smaller and elongated. At the lower electric potentials, gravitational forces determine dropping of the chitosan droplet, however, at the higher electric potential, electric potentials control the dropping process. Considering that the moment that the droplets were about to leave the tip of the needle toward the ground, it is very clear that the electric potential plays a critical role in controlling the morphology of CMs. Thus, as shown in Fig. 2, we could control the size of the CMs by adjusting the applied electric potentials: the higher electric potential applied, the smaller particle size was obtained. The electric potential also affected the dropping time of the chitosan droplets. Specifically, by gravitational force (0 kV), the droplet was dropped in 17.32 s while only 0.19 s was required at 10 kV. This consequently controlled particle sizes in reverse proportion to the applied electric potentials.

Unlike conventional electrospinning processes, the charged jets are curling into an aqueous phase, thus it is critical to monitor whether the whole portion of the ejected polymer solution can be hardened and fabricated to the solid microspheres. Table I shows the recovery yield of the CMs after the microspheres were hardened and lyophilized. When the chitosan solutions at 1% and 2% were electrospun, the recovery yields of all CMs were very high (>80%) except those at 10 kV. Too high electric potentials between the needle and the ground seemed to sputter the polymeric jets into finer droplets rather than microsized droplets. In fact, electrospinning processes at higher voltages (>10 kV) has been favorably employed in terms of fabrication nano-sized fibers due to increased sputtering of the charged jets (39,40). When the chitosan solution at 3% was electrospun, however, no difference was found according to the voltage changes. This can be clearly attributed that the viscosity of the chitosan solution is high enough to override the effect of electric fields; the formation of microspheres is rather dependent on gravitational forces and surface tension of the chitosan droplet at the needle (41,42).

Figure 4 shows the formation of CMs at various concentrations of chitosan solutions and various flow rates for electrospinning. When the solidified droplets of the chitosan solution was examined by light microscopy (Fig. 3a, inset), the microspheres were round-shaped; however, after freeze-drying, the overall size of the microspheres seemed to be collapsed and the morphology looks much like "football" rather than spheres. This is clearly caused by the higher electric potential (10 kV) applied to the system and coincides with

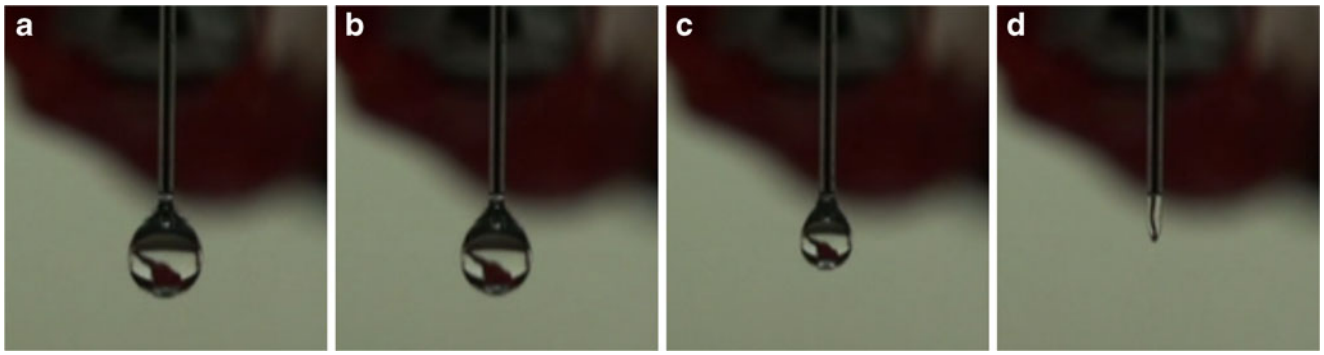

Fig. 3. Morphology of chitosan droplets at the tip of the injection needle at various electric potentials. Chitosan solutions (2%) were ejected at 2 ml/h and the formation of droplets was monitored by a digital video camcorder at 30 fps. All images are presented in a single picture frame that the droplets is about to leave the needle at the electric potentials of **a** 0.0 kV, **b** 2.5 kV, **c** 5.0 kV, and **d** 10.0 kV. The dropping time at the lower table was determined by analyzing the between period of the microspheres dropping (n=3)

the result of Fig. 2, which shows the elongation of the charged droplets at higher electric potentials (10 kV). The flow rate did not affect the average size of the CMs; the size of the electrospun microspheres is ranged from 200 to 400 μm. Interestingly, the size of the CMs was considerably decreased when the chitosan concentrations were decreased to 1%. We speculate that 1% chitosan solution was not viscous enough to form a droplet at the tip of the injection needle, thus premature droplets were ejected to the ground to form very fine particles. Thus, we conclude that more than 2% of chitosan concentration is required to obtain microspheres by electrospinning.

Table II shows the recovery yields of the CMs according to the chitosan concentration and the feeding rate of the chitosan solution for electrospinning. In all groups, the recovery yields did not significantly changed for the different parameters. However, when the feeding rate increased upto 4 ml/h, the recovery yields also increased with irrespective of chitosan concentrations: the recover yields ranged from 85.0% to 88.7% at 4.0 ml/h while those at 2 ml/h were 68.8% to 70.8%. When the droplet size at the needle increases due to the increased feeding rates, the mass of the curling jets also increased and larger particles can be consequently fabricated compared to those with lower feeding rates. Thus, the recovery yield of CMs is considerably increased due to the formation of large particles. However, it should be noticeable that the recovery yields of 3% chitosan concentration were steeply increased to 95.0% when the feeding rate was 0.5 ml/h. Due to the higher concentration and the lower feeding rate, we observed that the droplet formation at the needle was confirmed to be very slow (>70 s). Thus, evaporation of water occurs at

Table I. Recovery Yield (%, *w*/*w*) of CMs with Various Concentrations of Chitosan and Various Positive Voltage at 2 ml/h of Feeding Rate (n=3)

Concentration of chitosan (%, *w*/*v*)	Positive voltage (kV)		
	2.5	5.0	10.0
1.0	80.1±18.3	88.6±16.9	69.0±13.3
2.0	91.2±4.6	97.2±1.3	70.8±7.7
3.0	82.3±11.4	81.3±3.3	76.2±12.9

Recovery yield of CMs (%, *w*/*w*)=(the acquired amount of solidified CMs/the theoretical amount of CMs)×100

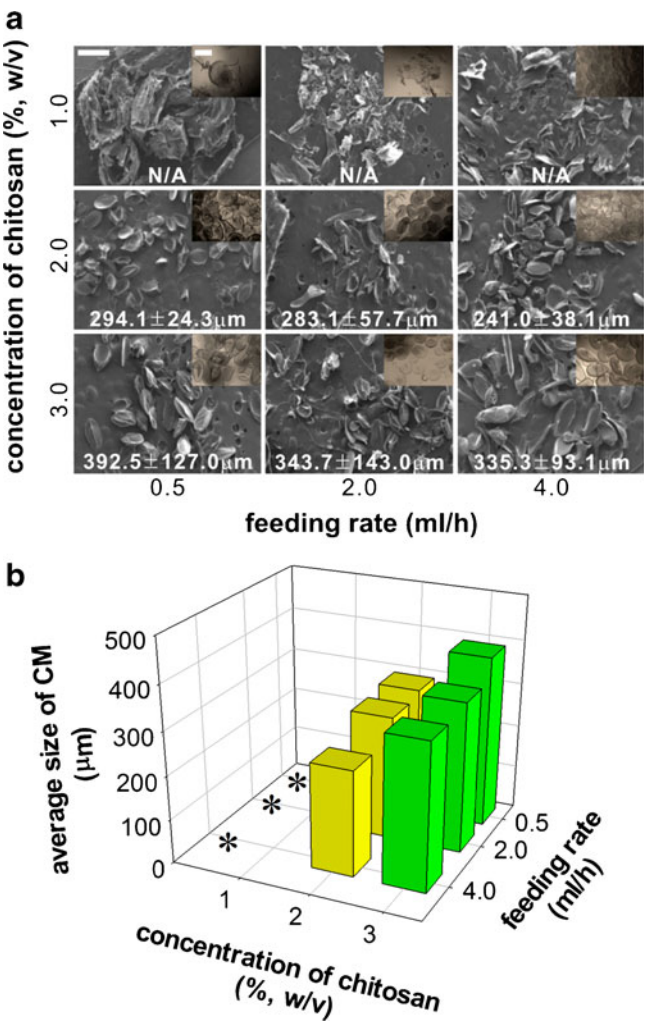

Fig. 4. Fabrication of CMs with various feeding rates and concentrations of chitosan solutions at 10 kV. **a** SEM of the CMs after solidification in 4.0 M Na_2CO_3. The *insets* are the optical microscopic images of the solidified CMs before lyophilization. **b** Average diameters of CMs based on an image analysis of the SEM images. The average diameters were plotted against the concentrations of chitosan solution and feeding rates changes (n=10). All *scale bars* in the images are 500 μm. *Asterisks* when chitosan concentration was 1% (*w*/*v*), the average sizes of CMs could not be measured because of irregular shapes of the CMs

Table II. Recovery Yield (%, *w*/*w*) of CMs with Various Concentrations of Chitosan and Various Feeding Rate at 10 kV of Positive Voltage (n=3)

Concentration of chitosan (%, *w*/*v*)	Feeding rate (ml/h)		
	0.5	2.0	4.0
1.0	70.1±10.2	69.0±13.3	88.7±8.5
2.0	60.4±8.2	70.8±7.7	85.0±12.1
3.0	95.0±29.5	76.2±12.9	87.0±24.3

Recovery yield of CMs (%, *w*/*w*)=(the acquired amount of solidified CMs/the theoretical amount of CMs)×100

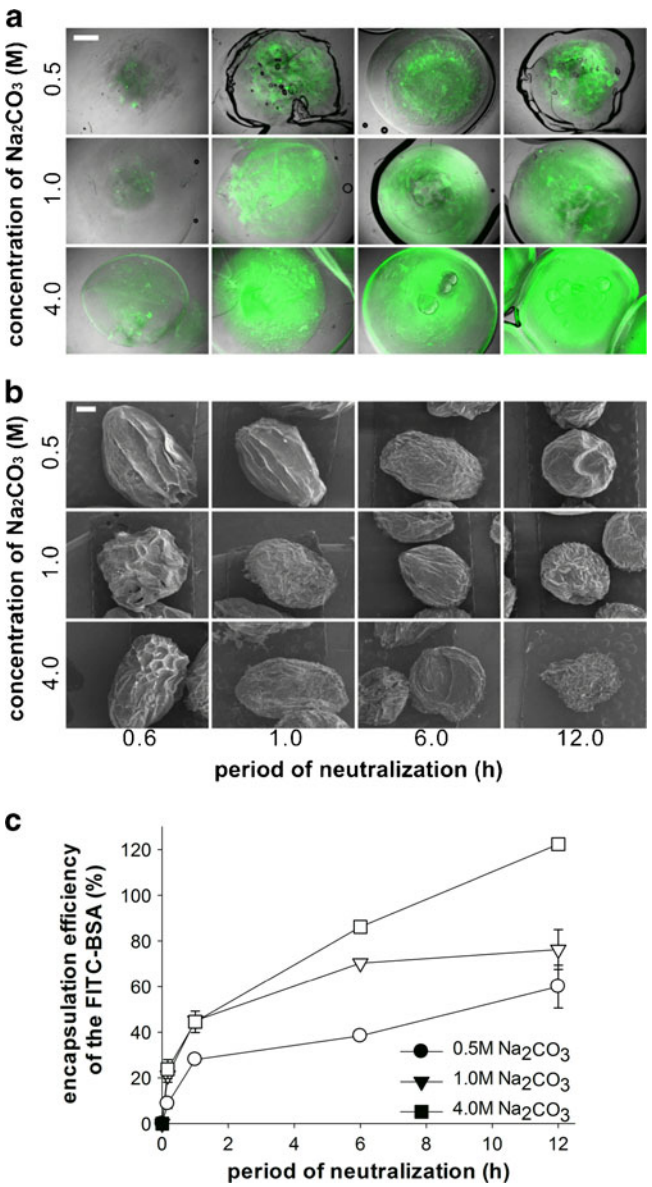

Fig. 5. Encapsulation of FITC–BSA in CMs with various concentrations of Na_2CO_3 and neutralization periods. **a** Confocal laser scanning microscopy images of the FITC–BSA encapsulated CMs at 2.0 ml/h of feeding rate and 2.5 kV. The FITC–BSA was shown in *green*. **b** SEM of the FITC–BSA encapsulated CMs after lyophilization and **c** encapsulation efficiencies of the FITC–BSA in the CMs by measuring the fluorescence intensity of the supernatant after centrifugation of solidified CMs. All *scale bars* are 500 μm

the prolonged retention time at the needle and the surface of the chitosan droplet is subsequently solidified due to increased concentration of the chitosan solution. The solidified droplets are gravitationally dropped into the receiver solution and the recovery yields are increased.

In order to evaluate CMs as protein eluting reservoirs, we encapsulated BSA in CMs by electrospinning protein-dissolved chitosan solutions. Figure 5a shows confocal microscopy of FITC–BSA encapsulating CMs, which were solidified in various concentrations of chitosan solutions for different periods. The fluorescence intensity of FITC–BSA was increased when the CMs were incubated in a higher concentration of Na_2CO_3 for a longer period of time. When the supernatant of the solidified microspheres were measured for the fluorescence intensity of unencapsulated FITC–BSA, the encapsulation efficiency were also dependent on the concentration and exposure time of the semi-solidified microspheres in Na_2CO_3 solution, which showed accordance with the visualization study of the FITC–BSA in Fig. 5a. In all concentrations of Na_2CO_3, the encapsulations of FITC–BSA were gradually increased when the exposure time to Na_2CO_3 increased up to 12 h. Among those, CMs incubated in 4.0 M Na_2CO_3 showed the highest encapsulation efficiency while those

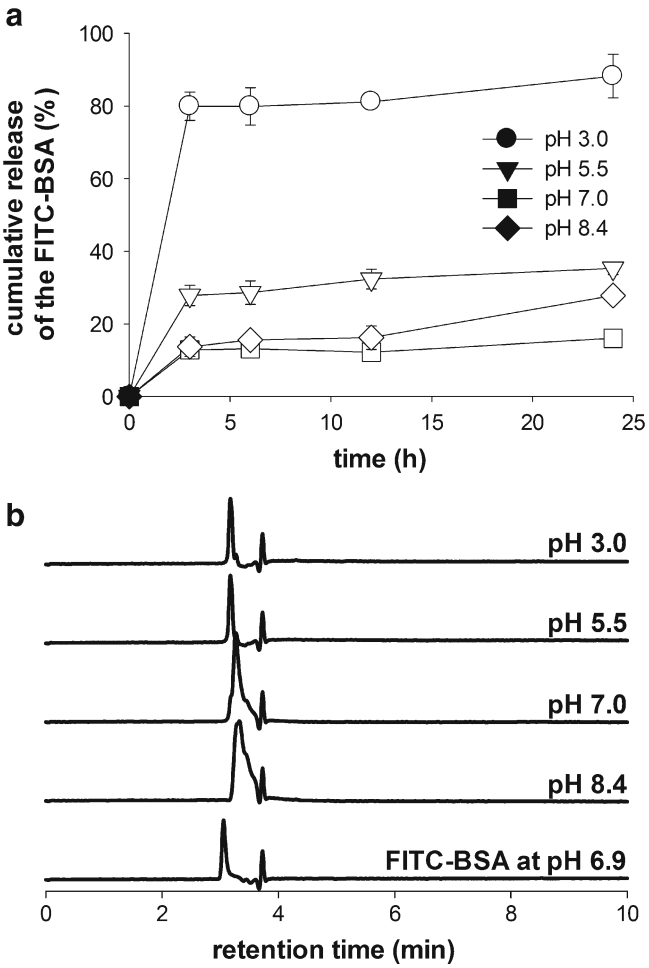

Fig. 6. Release study of FITC–BSA encapsulated CMs. Chitosan solution was electrospun at 10 kV, 2.0 ml/h of a feeding rate and solidified in 4.0 M Na_2CO_3 for 12 h. **a** Release profiles of FITC–BSA from the CMs at various pHs (pH 3.0, 5.5, 7.0, and 8.4). **b** Analysis of the released fractions of the CM by RP-HPLC. FITC–BSA at pH 6.9 was employed as a control

in 0.5 M Na_2CO_3 showed the lowest efficiency. Compared to other studies employing polymeric microspheres for protein encapsulation, our result clearly suggests that higher encapsulation efficiencies of the proteins can be accomplished with this strategy. This can be attributed to (1) uniqueness of the fabrication method of CMs and (2) electrostatic interactions between chitosan and anionic protein. Although some microspheres were previously fabricated by electrospinning as an alternative method for emulsification, polymeric solutions in organic solvents were only electrospun for fabrication of microspheres in those studies. Thus, water-soluble proteins dispersed in the organic solvents should experience denaturation and aggregation during the electrospinning. This subsequently causes irregular dispersion of proteins in the protein microspheres and the overall encapsulation efficiency can be considerably low (43,44). However, we herein proposed the electrospinning of chitosan solution and encapsulated BSA in the aqueous phase for electrospinning. Thus, the protein can be more homogeneously dispersed in the matrix of the microspheres and the protein encapsulation can be significantly increased. Moreover, the positively-charged chitosan can be effectively incorporated anionic BSA by electrostatic interactions, which also plays a significant role in withholding undesirable escape of protein during the solidification process of CMs (45,46). Chitosan/PEO–PPO nanoparticles containing BSA could control incorporation efficiency and release behavior of BSA due to the electrostatic interaction (45).

The release behaviors of the encapsulated FITC–BSA were investigated at various pH as shown in Fig. 6. In the incubation medium with lower pHs, the higher amounts of the encapsulated FITC–BSA were released out; thus *ca.* 80% of the encapsulated FITC–BSA were released out in 24 h when CMs were incubated at pH 3.0 while those at pH 7.0 only showed *ca.* 10% release of the encapsulated FITC–BSA. This can be clearly attributed to pH-dependent dissolution of chitosan comprising the microspheres. The solubility of chitosan increases in acidic solutions because the amine groups of the chitosan chains become protonated. This consequently induces complete degradation of CMs in a short period of time and the solution became clear when CMs were incubated at pH 3.0 (data not shown). Additionally, we analyzed the released fractions by RP-HPLC to verify whether any structural modification of the encapsulate FITC–BSA at each pH. Because protein in CMs experienced extreme change of pH from low pH (acetic acid) to high pH (sodium carbonate), which may result in irreversible structural changes such as deamidation (47). Subsequent changes of net-charges can be usually evaluated by reversed-phase chromatography because any changes of single amine acid is directly associated with the hydrophobicity of the protein while CD and SDS-PAGE cannot detect such a minute change. Also, the net charges of the released BSA can be slightly changed at pH 7.0 and 8.5 than lower pHs by the chemical changes of the protein structure, resulting in peak broadening appeared on the chromatograms as the higher pHs. The deamidation of the amine acids containing amine side chains can be the one of the underlying mechanism for such changes because the deamidation reaction proceeds quickly at the elevated pHs. Figure 6b clearly indicates that there was no change in the RP-HPLC profile at all pHs, suggesting that the two-dimesional structure of the FITC–BSA was not changed at low pHs. This result clearly shows that CMs can be potentially applied for protein carriers in aim to control release of the encapsulated protein according to pH changes.

CONCLUSION

Electrospinning parameters such as electric potentials and feeding rates affected the morphology and size of the chitosan microspheres. Especially, when a concentration of chitosan solution was 2.0~3.0%, the morphology and size of the chitosan microspheres were optimized with 5.0~10.0 kV of electric potentials and 2.0 ml/h of feeding rate. Solidification and protein encapsulation of microspheres was dependent on the concentration of sodium carbonate solution and the exposure time to the solution. Especially, the optimized conditions for the solidification were 4.0 M sodium carbonate and above 6 h of the exposure time. Release rates of the encapsulated protein were increased at lower pH and the stability of the released protein was confirmed by HPLC analysis.

ACKNOWLEDGMENTS

This work was supported by the grant from the National Research Foundation (grant #: 2012000717R1A1A2) and the leaders in Industry–University Cooperation (LINC) program of Kangwon National University funded by the Ministry of Education, Science, and Technology, Republic of Korea. We thank Eunju Jo for technical assistance.

REFERENCES

1. Zhu G, Mallery SR, Schwendeman SP. Stabilization of proteins encapsulated in injectable poly (lactide-*co*-glycolide). Nat Biotechnol. 2000;18:52–7.
2. Okada H, Heya T, Igari Y, Ogawa Y, Toguchi H, Shimamoto T. One-month release injectable microspheres of leuprolide acetate inhibit steroidogenesis and genital organ growth in rats. Int J Pharm. 1989;54:231–9.
3. Jain RA, Rhodes CT, Raikar AM, Malick AW, Shah NH. Controlled release of drugs from injectable *in situ* formed biodegradable PLGA microspheres: effect of various formulation variables. Eur J Pharm Biopharm. 2000;50:257–62.
4. Yan C, Resau JH, Hewetson J, West M, Rill WL, Kende M. Characterization and morphological analysis of protein-loaded poly (lactide-*co*-glycolide) microparticles prepared by water-in-oil-in-water emulsion technique. J Control Release. 1994;32:231–41.
5. Lemoine D, Wauters F, Bouchend'homme S, Preat V. Preparation and characterization of alginate microspheres containing a model antigen. Int J Pharm. 1998;176:9–19.
6. Prottey C, Ferguson TFM. The effect of surfactants upon rat peritoneal mast cells *in vitro*. Food Cosmet Toxicol. 1976;14:425–30.
7. Ernst R, Arditti J. Biological effects of surfactants. IV. Effects of nonionics and amphoterics on hela cells. Toxicology. 1980;15:233–42.
8. Baimark Y. Preparation of organic solvent/surfactant-free microspheres of methoxy poly(ethylene glycol)-*b*-poly(ε-caprolactone) by a melt dispersion method. Asian J Appl Sci. 2009;2:341–7.
9. Li JK, Wang N, Wu XS. Gelatin nanoencapsulation of protein/peptide drugs using an emulsifier-free emulsion method. J Microencapsul. 1998;15:163–72.
10. Sebti T, Amighi K. Preparation and *in vitro* evaluation of lipidic carriers and fillers for inhalation. Eur J Pharm Biopharm. 2006;63:51–8.
11. Bittner B, Mader K, Kroll C, Borchert HH, Kissel T. Tetracycline-HCl-loaded poly($_{DL}$-lactide-co-glycolide) microspheres prepared by a spray drying technique: influence of g-irradiation on radical formation and polymer degradation. J Control Release. 1999;59:23–32.
12. Sashiwa H, Aiba S. Chemically modified chitin and chitosan as biomaterials. Prog Polym Sci. 2004;29:887–908.

13. Dutta PK, Dutta J, Tripathi VS. Chitin and chitosan: chemistry, properties and applications. J Sci Ind Res. 2004;63:20–31.
14. Wang YC, Lin MC, Wang DM, Hsieh HJ. Fabrication of a novel porous PGA-chitosan hybrid matrix for tissue engineering. Biomaterials. 2003;24:1047–57.
15. Kast CE, Frick W, Losert U, Schnurch AB. Chitosan-thioglycolic acid conjugate: a new scaffold material for tissue engineering. Int J Pharm. 2003;256:183–9.
16. Pillai CKS, Paul W, Sharma CP. Chitin and chitosan polymers: chemistry, solubility and fiber formation. Prog Polym Sci. 2009;34:641–78.
17. Mi FL, Sung HW, Shyu SS. Release of indomethacin from a novel chitosan microsphere prepared by a naturally occurring crosslinker: examination of crosslinking and polycation-anionic drug interaction. J Appl Polym Sci. 2001;81:1700–11.
18. Wang LY, Gu YH, Zhou QZ, Ma GH, Wan YH, Su ZG. Preparation and characterization of uniform-sized chitosan microspheres containing insulin by membrane emulsification and a two-step solidification process. Colloids Surf B Biointerfaces. 2006;50:126–35.
19. He P, Davis SS, Illum L. Chitosan microspheres prepared by spray drying. Int J Pharm. 1999;187:53–65.
20. Muzzarelli C, Stanic V, Gobbi L, Tosi G, Muzzarelli RAA. Spray-drying of solutions containing chitosan together with polyuronans and characterization of the microspheres. Carbohydr Polym. 2004;57:73–82.
21. Desai KG, Park HJ. Effect of manufacturing parameters on the characteristics of vitamin C encapsulated tripolyphosphate-chitosan microspheres prepared by spray-drying. J Microencapsul. 2006;23:91–103.
22. Buttafoco L, Kolkman NG, Engbers-Buijtenhuijs P, Poot AA, Dijkstra PJ, Vermes I, *et al*. Electrospinning of collagen and elastin for tissue engineering application. Biomaterials. 2006;25:724–34.
23. Lee S, Obendorf SK. Use of electrospun nanofiber web for protective textile materials as barriers to liquid penetration. Text Res. 2007;77:696–702.
24. Yoshimoto H, Shin YM, Terai H, Vacanti JP. A biodegradable nanofiber scaffold by electrospinning and its potential for bone tissue engineering. Biomaterials. 2003;24:2077–82.
25. Cui W, Li X, Zhu X, Yu G, Zhou S, Weng J. Investigation of drug release and matrix degradation of electrospun poly($_{DL}$-lactide) fibers with paracetanol inoculation. Macromolecules. 2006;7:1623–9.
26. Choi JS, Leong KW, Yoo HS. *In vivo* wound healing of diabetic ulcers using electrospun nanofibers immobilized with human epidermal growth factor (EGF). Biomaterials. 2008;29:587–96.
27. Choi JS, Yoo HS. Nano-inspired fibrous matrix with bi-phasic release of proteins. J Nanosci Nanotechnol. 2010;10:3038–45.
28. Cho YI, Choi JS, Jeong SY, Yoo HS. Nerve growth factor (NGF)-conjugated electrospun nanostructures with topographical cues for neuronal differentiation of mesenchymal stem cells. Acta Biomater. 2010;6:4725–33.
29. Sanders EH, Kioefkorn R, Bowlin GL, Simpson DG, Wnek GE. Two-phase electrospinning from a single electrified jet: microencapsulation of aqueous reservoirs in poly(ethylene-*co*-vinyl acetate) fibers. Macromolecules. 2003;36:3803–5.
30. Kim SE, Park JH, Cho YW, Chung H, Jeong SY, Lee EB, *et al*. Porous chitosan scaffold containing microspheres loaded with transforming growth factor- β1: Implications for cartilage tissue engineering. J Control Release. 2003;91:365–74.
31. Schiffman JD, Stulga LA, Schauer CL. Chitin and chitosan: transformations due to the electrospinning process. Polym Eng Sci. 2009;49:1918–28.
32. Sangsanoh P, Supaphol P. Stability improvement of electrospun chitosan nanofibrous membranes in neutral or basic aqueous solutions. Biomacromolecules. 2006;7:2710–4.
33. Thompson CJ, Chase GG, Yarin AL, Reneker DH. Effect of parameters on nanofiber diameter determined from electrospinning model. Polymer. 2007;48:6913–22.
34. Lee HW, Karin MR, Ji HM, Choi JH, Ghim HD, Park SM, *et al*. Electrospinning fabrication and characterization of poly(vinyl alcohol)/montmorillonite nanofiber mats. J Appl Polym Sci. 2009;113:1860–7.
35. Geng X, Kwon OH, Jang J. Electrospinning of chitosan dissolved in concentrated acetic acid solution. Biomaterials. 2005;26:5427–32.
36. Katti DS, Robinson KW, Ko FK, Laurencin CT. Bioresornanle nanofiber-based systems for wound healing and drug delivery: optimization of fabrication parameters. Biomed Mater Res B Appl Biomater. 2004;70:286–96.
37. Son B, Yeom BY, Song SH, Lee CS, Hwang TS. Antibacterial electrospun chitosan/poly(vinyl alcohol) nanofibers containing silver nitrate and titanium dioxide. J Appl Polym Sci. 2008;111: 2892–9.
38. Ohsawa O, Lee KH, Kim BS, Lee S, Kim IS. Preparation and characterization of polyketone (PK) fibrous membrane *via* electrospinning. Polymer. 2010;51:2007–12.
39. Choi JS, Yoo HS. Eletrospun nanofibers surface-modified with fluorescent proteins. J Bioact Compat Polym. 2007;22:508–24.
40. Kim HS, Yoo HS. MMPs-responsive release of DNA from electrospun nanofibrous matrix for local gene therapy: *in vitro* and *in vivo* evaluation. J Control Release. 2010;145:264–71.
41. Mo XM, Xu CY, Kotaki M, Ramakrishna S. Electrospun P(LLA-CL) nanofiber: a biomimetic extracellular matrix for smooth muscle cell and endothelial cell proliferation. Biomaterials. 2004;25:1883–90.
42. Ding B, Kim HY, Lee SC, Lee DR, Choi KJ. Preparation and characterization of nanoscaled poly(vinyl alcohol) fibers *via* electrospinning. Fiber Polym. 2002;3:73–9.
43. Carrasquillo KG, Stanley AM, Aponte-Carro JC, Jesus PD, Costantino HR, Bosques CJ, *et al*. Non-aqueous encapsulation of excipient-stabilized spray-freeze dried BSA into poly(lactide-*co*-glycolide) microspheres results in release of native protein. J Control Release. 2001;76:199–208.
44. Crotts G, Park TG. Preparation of porous and nonporous biodegradable polymeric hollow microspheres. J Control Release. 1995;35:91–105.
45. Calvo P, Remuflan-Lopez C, Vila-Jato JL, Alouso MJ. Chitosan and chitosan/ethylene oxide-propylene oxide block copolymer nanoparticles as novel carriers for proteins and vaccines. Pharm Res. 1997;14:1431–6.
46. Yu CY, Yin BC, Zhang W, Cheng SX, Zhang XZ, Zhuo RX. Conposite microparticle drug delivery systems based on chitosan, alginate and pectin with improved pH-sensitive drug release property. Colloids Surf B Biointerfaces. 2009;68:245–9.
47. Nold MJ, Wesdemiotis C, Yalcin T, Harrison AG. Amide bond dissociation in protonated peptides. Structures of the *N*-terminal ionic and neutral fragments. Int J Mass Spectrom Ion Process. 1997;164:137–53.